Application of bubble-check algorithm to non-binary LLR computation in QAM coded schemes

L. Conde-Canencia and E. Boutillon

The generation of intrinsic LLR messages in non-binary (NB) coded schemes associated with quadrature amplitude modulation (QAM) is considered. It is shown that the intrinsic LLR message generation corresponds to the same kind of computation as the one performed at the elementary check nodes in extended min-sum NB-LDPC decoders, i.e. finding a given number of minimum values in a structured set. It is proposed to use the bubble-check algorithm for the LLR calculation to benefit from two advantages: low-complexity hardware architecture and sharing the same hardware at the demapping and the decoding steps.

Introduction: Non-binary (NB)-coded schemes can be naturally associated with high-order modulation for a high data rate, leading to low-error high-spectral-efficiency communication systems. Compared with binary coded schemes, the use of NB codes improves the performance of decoding algorithms [1, 2] as the intrinsic likelihoods of the received symbols (which are the inputs to the decoder) are uncorrelated from one symbol to another. Recent work on quadrature amplitude modulation (QAM) binary soft demapping includes that in [3].

Fig. 1 presents the schematics of the considered digital communication chain. Information data are encoded by an NB encoder and then mapped to a symbol in the QAM constellation. Note that the order of the NB code, q, corresponds to the number of signals in the modulation, M (i.e. $M = q$). After the channel, the modulated noisy symbols are demapped to generate the intrinsic message. Note that this Letter focuses on the demapper block and considers the generation of the intrinsic likelihood messages. Even if our approach may be considered for any NB-coded modulation scheme that needs the sorting of elements in the likelihood vector, we essentially focus on NB-LDPC and extended min-sum (EMS) [4] decoding algorithms. [The min-max [5] decoding algorithm would also fit in our study.]

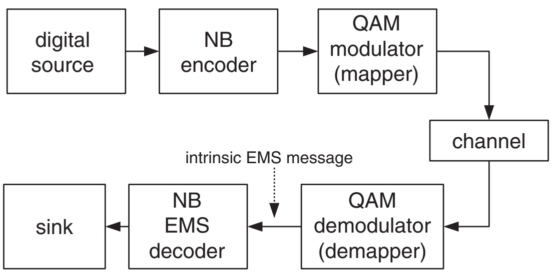

Fig. 1 *Digital communication chain*

NB-coded modulation: Let $\boldsymbol{X} = (x_1, x_2, \ldots, x_N)$ be the codeword generated by the NB encoder, where x_k is an element of GF(q), i.e. $x_k = a_p$, $p = 0, \ldots, q-1$. Let C be the mapping of the set GF(q) to the set of points of the constellation (each point represents a modulation signal): $C{:}a_p \in \mathrm{GF}(q) \to (\pi_I(p), \pi_Q(p))_{p=0,1,2,\ldots,q-1} \in M-\mathrm{QAM}$. In other words, the 2^m-ary QAM (where m is even) is decomposed into two independent $2^{m/2}$-ary pulse amplitude modulations (PAMs). For each a_p, the I coordinate corresponds to the in-phase axis ('idem' Q coordinate, in-quadrature axis).

The received noisy codeword $\boldsymbol{Y}$ consists of N NB symbols independently affected by noise. Each symbol is represented by $y_k = C(x_k) + w_k$, $k \in \{1, 2, \ldots, N\}$, w_k is the realisation of a complex additive white Gaussian noise (AWGN) of variance σ^2.

EMS decoding algorithm: The EMS algorithm was proposed for NB-LDPC low-complexity decoding in [4, 6] as a generalisation of the min-sum algorithm used for binary LDPC codes [7–9]. Its principle is the truncation of the vector messages from q to n_m values ($n_m \ll q$). The complexity/performance trade-off can be adjusted with the value of the n_m parameter. This characteristic makes the EMS decoder architecture easily adaptable to both implementation and performance constraints.

EMS intrinsic message: For each received symbol y_k, the intrinsic message is composed of n_m couples, each one containing a log-likelihood ratio, L_i, and its associated GF(q) symbol, a_i, i.e. $(L_i, a_i)_{i \in 1,\ldots,n_m}$ where $L_1 \le L_2 \le \cdots \le L_{n_m}$. In the following, index k is omitted ($y = y_k$). Each L_i is defined as

$$L_i = ln\left(\frac{P(y|\tilde{a})}{P(y|a_i)}\right) = \frac{d^2(C(a_i), y_k) - d^2(C(\tilde{a}), y_k)}{2\sigma^2} \quad (1)$$

where $\tilde{a}$ is the GF(q) symbol associated with the nearest point to y in the QAM constellation, i.e. the one that maximises $P(y|a_i)$ for $i \in (1, \ldots, n_m)$. The Euclidean distance between two points in signal space is represented by $d()$.

Demapper: The function of the demapper is to generate the intrinsic message for each received symbol y_k. For the sake of simplicity, let $d_i^2 = d^2(a_i, y)$ and $\delta^2 = d^2(\tilde{a}, y)$. Moreover, $d_i^2 = d_{iI}^2 + d_{iQ}^2$ and $\delta^2 = \delta_I^2 + \delta_Q^2$ as we decompose the M-QAM into two $2^{m/2}$-ary PAMs for distance calculation. Then, we can write

$$\underbrace{d_i^2 - \delta_i^2}_{2\sigma^2 L_i} = \underbrace{(d_{iI}^2 - \delta_I^2)}_{U(i)} + \underbrace{(d_{iQ}^2 - \delta_Q^2)}_{V(i)} \quad (2)$$

Finally, the objective is to select the n_m smallest distances (sorted in increasing order) and their associated symbols a_i, in order to generate the intrinsic EMS message for y.

Finding the minimum distances with the bubble-check algorithm: In [10], Boutillon and Conde-Canencia presented a low-complexity algorithm for extracting n_m minimum values in the set defined as $U(i) + V(j)$, $(i, j) \in [1, n_m]^2$. This set is represented as a matrix T_Σ, where $T_\Sigma = U(i) + V(j)$. The elements in $\boldsymbol{U} = [U(1), U(2), \ldots, U(n_m)]$ and $\boldsymbol{V} = [V(1), V(2), \ldots, V(n_m)]$ are sorted in increasing order. Then, we can directly apply the bubble-check algorithm to generate the intrinsic message, as illustrated in Fig. 2.

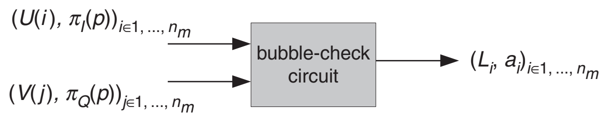

Fig. 2 *Application of bubble-check circuit to generate LLR intrinsic message*

Example for $M = q = 64$ and $n_m = 8$: Let us consider the case of a 64-QAM associated with a GF(64)-LDPC code with a Gray mapping as in the IEEE.802.11 standard (Fig. 4). Let $\boldsymbol{G}$ be $[-7, -5, -1, -3, 7, 5, 1, 3]$, then $\pi_I(p) = \boldsymbol{G}[\lfloor p/8 \rfloor]$ and $\pi_Q(p) = \boldsymbol{G}[p \bmod 8]$. This way $C(a_{52}) = (\boldsymbol{G}(6), \boldsymbol{G}(4)) = (+1, +7)$ or $C(a_{32}) = (\boldsymbol{G}(4), \boldsymbol{G}(0)) = (+7, -7)$.

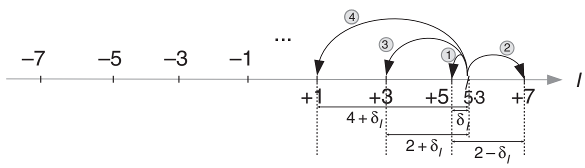

Fig. 3 *Sequential distance computation on I-axis*

Table 1: Distance computation on I-axis

i	$\pi_I(p)$	$\lfloor p/8 \rfloor$	d_{iI}^2	$U(i)$
1	+5	5	δ_I^2	0
2	+7	4	$4 + \delta_I^2 - 4\delta_I$	2.8
3	+3	7	$4 + \delta_I^2 + 4\delta_I$	5.2
4	+1	6	$16 + \delta_I^2 + 8\delta_I$	18.4
…	…	…	…	…

Let us now illustrate the demapping with the example that the received noisy signal is $y = (5.3, -3.2)$. Then, $C(\tilde{a}) = (+5, -3)$ and $\delta^2 = 0.3^2 + 0.2^2$. Let us focus first on the I-axis. The calculation of the sorted values in $U(i)$ can be performed with a state machine

(Fig. 3 and Table 1) to obtain

$$(\mathbf{U}(i),\ \pi_I(p)) = \{(0,\ +5),\ (2.8,\ +7),\ (5.2,\ +3),\ (18.4,\ +1),\ \ldots\} \quad (3)$$

The same procedure for the Q-axis generates

$$(\mathbf{V}(j),\ \pi_Q(p)) = \{(0,\ -3),\ (3.2,\ -5),\ (4.8,\ -1),\ (14.4,\ -7),\ \ldots\} \quad (4)$$

Finally, Table 2 illustrates the generation of the EMS intrinsic message $(L_i,\ a_i)_{i\in(1,\ldots,n_m)}$ through the bubble-check circuit (Fig. 2). For $n_m = 8$, the intrinsic messages are $(0,\ a_{43})$, $(2.8,\ a_{35})$, $(3.2,\ a_{41})$, $(4.8,\ a_{42})$, $(5.2,\ a_{59})$, $(6,\ a_{33})$, $(7.6,\ a_{34})$ and $(8.4,\ a_{57})$ which correspond to the n_m closest signals to y.

Table 2: Application of bubble-check algorithm

$(V(j),\ \pi_Q(p))$	$(U(i),\ \pi_I(p))$			
	$(0,\ +5)$	$(2.8,\ +7)$	$(5.2,\ +3)$	$(18.4,\ +1)$
$(0,\ -3)$	$(L_1 = 0,\ a_{43})$	$(L_2 = 2.8,\ a_{35})$	$(L_3 = 5.2,\ a_{59})$	18.4
$(3.2,\ -5)$	$(L_3 = 3.2,\ a_{41})$	$(L_6 = 6,\ a_{33})$	$(L_8 = 8.4,\ a_{57})$	21.6
$(4.8,\ -1)$	$(L_4 = 4.8,\ a_{42})$	$(L_7 = 7.6,\ a_{34})$	10	23.2
$(14.4,\ -7)$	14.4	17.2	19.6	32.8
…	…	…	…	…

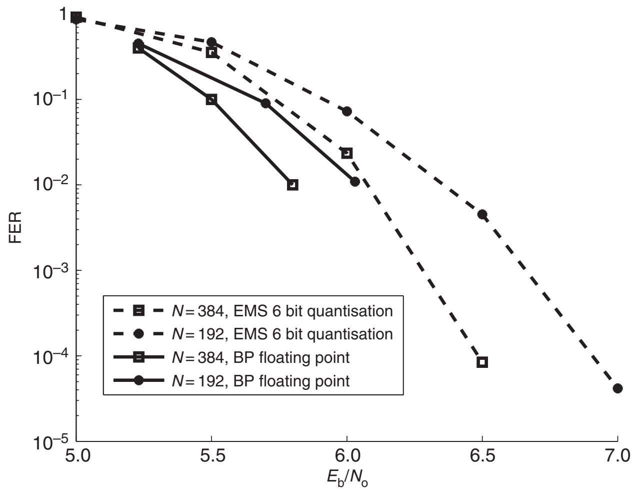

Fig. 4 *Performance comparison of BP and EMS for GF(64)-LDPC associated with 64-QAM*

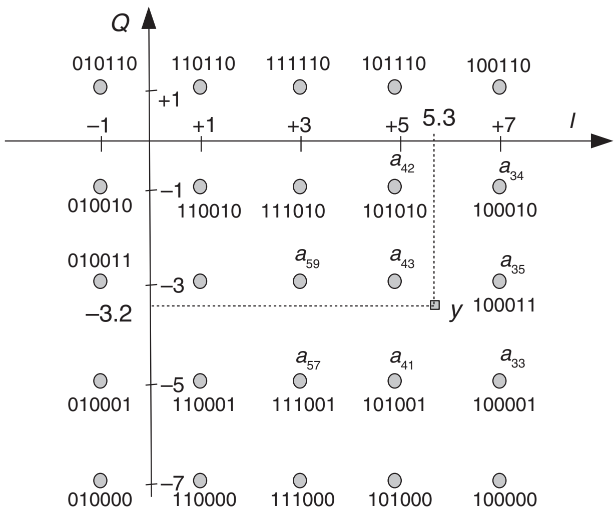

Fig. 5 *Zoom on 64-QAM constellation and n_m closest points to y for EMS intrinsic message generation*

Results: Fig. 4 presents the simulation results obtained for the ultra-sparse protograph-based NB-LDPC on GF(64) associated with a 64-QAM as in Fig. 5 for frame sizes of $N = 192$ symbols (1152 bits) and $N = 384$ (2304 bits) with a code rate of 1/2 over the AWGN channel. The BP curves correspond to the belief propagation decoding, simulated on the floating point with 100 decoding iterations (see [11]). The EMS curves consider the EMS NB-LDPC decoder described in [12] with $n_m = 12$, 20 decoding iterations, 6 bit quantisation [note that this decoder design was implemented on a field programmable gate array (FPGA) [12]] and the intrinsic LLR generation presented in this Letter. A performance gap of about 0.4 dB is observed between the BP and EMS curves, which confirms the interest of our approach from both the performance and the low-complexity implementation aspect.

Conclusion: This Letter focuses on low-complexity intrinsic LLR generation for high-order NB-coded QAM designs. The originality is in the use of the bubble-check algorithm for the computation of the intrinsic message. The simulation results show the interest of this work in terms of performance. The FPGA implementation of the NB-LDPC EMS decoder and the bubble-check architecture design considered in [12] is proof of the implementation feasibility of both the QAM demodulator and the decoder (Fig. 1).

Acknowledgment: This work was supported by the PALMYRE project and INFSCO-ICT-216203 DAVINCI 'Design And Versatile Implementation of Non-binary wireless Communications based on Innovative LDPC Code' (http://www.ict-davinci-codes.eu) funded by the European Commission under the Seventh Framework Program (FP7). The authors thank O. Abassi for helpful discussion and results.

1 August 2014
doi: 10.1049/el.2014.2652

L. Conde-Canencia and E. Boutillon (*Lab-STICC Laboratory, CNRS UMR 6285, UBS, Lorient, France*)

E-mail: laura.conde-canencia@univ-ubs.fr

References

1 Sridhara, D., and Fuja, T.: 'Low density parity check codes defined over groups and rings'. Proc. Inf. Theory Workshop, Bangalore, India, October 2002
2 Declercq, D., Colas, M., and Gelle, G.: 'Regular GF(2^q)-LDPC coded modulations for higher order QAM-AWGN channel'. Proc. ISITA, Parma, Italy, October 2004
3 Wang, Q., Xie, Q., Wang, Z., Chen, S., and Hanzo, L.: 'A universal low-complexity symbol-to-bit soft demapper', *IEEE Trans. Veh. Technol.*, 2014, **63**, (1), pp. 119–130
4 Declercq, D., and Fossorier, M.: 'Decoding algorithms for nonbinary LDPC codes over GF(q)', *IEEE Trans. Commun.*, 2007, **55**, (4), pp. 633–643
5 Savin, V.: 'Min–max decoding for non binary LDPC codes'. ISIT 2008 IEEE Int. Symp. on Information Theory, Toronto, Canada, July 2008, pp. 960–964
6 Voicila, A., Declercq, D., Verdier, F., Fossorier, M., and Urard, P.: 'Low complexity, low memory EMS algorithm for non-binary LDPC codes'. IEEE Int. Conf. on Communications, ICC'2007, Glasgow, UK, June 2007
7 Zhao, J., Zarkeshvari, F., and Banihashemi, A.H.: 'On implementation of min-sum algorithm and its modifications for decoding LDPC codes', *IEEE Trans. Commun.*, 2005, **53**, (4), pp. 549–554
8 Fossorier, M., Mihaljevi, M., and Imai, H.: 'Reduced complexity iterative decoding of LDPC codes based on belief propagation', *IEEE Trans. Commun.*, 1999, **47**, p. 673
9 Kschischang, F., Frey, B., and Loeliger, H.-A.: 'Factor graphs and the sum product algorithm', *IEEE Trans. Inf. Theory*, 2001, **47**, (2), pp. 498–519
10 Boutillon, E., and Conde-Canencia, L.: 'Bubble-check: a simplified algorithm for elementary check node processing in extended min–sum non-binary LDPC decoders', *Electron. Lett.*, 2010, **46**, pp. 633–634
11 Bas, J., Bacci, G., Bourdoux, A., *et al.*: 'Link level evaluation, issue 1'. INFSCO-ICT-216203 DAVINCI D2.2.1. Avalaible at http://www.ict-davincicodes.eu/project/deliverables/D221.pdf, December 2008, pp. 1–24
12 Boutillon, E., Conde-Canencia, L., and Ghouwayel, A.A.: 'Design of a GF(64)-LDPC decoder based on the EMS algorithm', *IEEE Trans. Circuits Syst. I*, 2013, **60**, pp. 2644–2656